



Energy of electrons at the interaction of femtosecond laser with argon nanocluster

HOSSEIN GHAFORYAN

Department of Optics and Laser Engineering, University of Bonab, Bonab 5551761167, Iran
E-mail: drghaforyan@gmail.com

MS received 26 March 2018; revised 30 July 2018; accepted 4 October 2018;
published online 23 March 2019

Abstract. The interaction of intense femtosecond laser pulses with argon nanoclusters is studied using nanoplasma model. Based on the dynamic simulations, ionisation process, heating, and expansion of an argon nanocluster irradiated by an intense femtosecond laser pulse are investigated. The analytical calculation provides ionisation rate for different mechanisms and time evolution of hydrodynamic pressure for various pulse shapes. In this work, the dependence of laser intensity, initial ion density and pulse shape on the electron pressure, the density of electrons and electron temperature are presented. It is noticed that the negative and positive chirped pulses and initial ion density implement some modifications on the current calculation models. It is found that reducing the initial ion density at a laser intensity of about $1 \times 10^{16} \text{ W/hboxcm}^2$ increases the energy of electrons. By applying a positive chirp laser pulse during interaction with nanoclusters, both electron density and ultimately electron pressure are improved by about 22%.

Keywords. Nanocluster; electron pressure; nanoplasma; electron acceleration; electron density.

PACS Nos 42.65.-k; 42.65.Re; 52.38.Hb

1. Introduction

The current developments of ultrashort intense laser pulses using chirped pulse amplification (CPA) and optical parametric chirped pulse amplification (OPCPA) techniques have attracted increasing attention in laser-matter interaction [1]. Such pulses are used for the generation of quasimonoenergetic electron beams to mega-electron volts [2] and hard X-rays photons. The generated ponderomotive force in the plasma accelerates electrons of plasma to the relativistic energies over several MeV. In recent years, considerable progress has been made in increasing the energy and quality of electron beams, both theoretically and experimentally [3–5]. High-energy electrons can be used in fast ignition of fusion reaction, production of intense radiation sources such as X-ray, biological and medical technology [6–10]. Optimisation and control of this new source of energetic particles which can be modified by unique attractive techniques with different applications is an important subject for researchers. Interaction of intense laser pulses with large atomic nanoclusters is one of the most efficient methods that has opened up several areas of laser plasma science such as electron and ion accelerators [11–13], table-top neutron sources [14], plasma

waveguides [15], and X-ray sources [16]. Simulation of this interaction provides a suitable context for further research. Particle acceleration is one of the most important applications of laser-cluster interaction. Low price and the need for less space for the laser-plasma accelerators compared to other accelerators has led to more attention to this type of accelerators.

Nanoclusters have unique properties because they can act as both gas and solid. The transmission distance of the laser pulse in the cluster is longer than that in the gas target. Likewise, the absorbed laser energy in the cluster is larger than that of the solid and gas targets [17].

At this interaction, a nanocluster with 10000 atoms or more is called a nanoplasma sphere. The nanoplasma model was developed in 1996 by Ditmire and his colleagues [18]. This model successfully justifies all phenomena in the interaction. At this simulation, several improvements have been made which are in good agreement with the experiments [19].

In this article, we intend to modify the simulation of the dynamics of laser-cluster interaction. The aim is to improve the acceleration of electrons by considering optimised initial conditions of interaction. Initial ion density, laser intensity and laser pulse shapes are important parameters for the production of highly energetic

electrons. Another feature of this work is to study the ionisation rate for different mechanisms, hydrodynamic pressure on different pulse shapes, different intensity of laser pulse and different initial ion density. When positively chirped laser pulse is used, hydrodynamic electron pressure is improved by about 20% compared to Gaussian pulse. In this calculation, the argon cluster radius is considered to be 15 nm, the peak intensity of the laser is about 10^{16} W cm⁻², pulse duration (FWHM) is 40 fs and wavelength is 825 nm.

This paper is organised as follows: in §2, the theory of cluster formation and laser–cluster interaction including ionisation, heating, expansion of the cluster and also the ponderomotive force are described. In §3, the simulation results are explained in detail and the paper is concluded in §4.

2. Methods

2.1 Cluster formation

Clusters can be formed inside a high-pressure gas jet. When gas expands out of a nozzle into the vacuum, its random thermal energy is converted into kinetic energy of the gas flow. This adiabatic expansion quickly cools the gas atoms or molecules. Then, under specified conditions, they can be held together by the van der Waals force to condense into clusters. The degree of clustering and hence the size of a cluster is determined by the atomic species, the backing pressure, the stagnation temperature, and the geometry of the nozzle. The properties of the cluster medium are remarkable. Clusters such as gases have low average density but in some cases have near solid density. Clustering and the size of the clusters produced can be described by an empirical scaling parameter, Γ^* , known as the Hagena parameter [20]:

$$\Gamma^* = k \frac{(d/\tan \alpha)^{0.85} P_0}{T^{2.29}}. \quad (1)$$

Here d is the diameter of the nozzle, α is the jet expansion half angle, T is the temperature of the gas before expansion in kelvin, P_0 is the backing pressure of the jet in mbar, k is the condensation parameter which depends on the species of the atom.

Research has shown that clustering begins when $\Gamma^* \geq 300$. It is possible to control the value of Γ^* to engineer a cluster medium of arbitrary average density and cluster size by varying T and P_0 . The average number of atoms in each cluster is estimated as

$$n = 33 \times \left[\frac{\Gamma^*}{1000} \right]^q. \quad (2)$$

Here $q \approx 2-2.5$, which implies $n \approx P_0^{2-2.5}$. For $\Gamma^* \leq 10^4$, the average number of atoms per cluster is estimated from the following equation:

$$n = 33 \times \left[\frac{\Gamma^*}{1000} \right]^{2.35} \quad (3)$$

while for $\Gamma^* \gg 10^4$, the scaling law is modified to

$$n = 100 \times \left[\frac{\Gamma^*}{1000} \right]^{1.8}. \quad (4)$$

2.2 Short pulse interaction with nanocluster

Various models such as ionisation ignition model [21], the Coulomb explosion model [22], the inner shell excitation models [23], and nanoplasma models [24] are introduced. The most successful method for checking the dynamical evolution of large clusters under intense femtosecond laser radiation is the nanoplasma model in which three main processes, ionisation, heating, and expansion, exist. The dynamics of the laser–cluster interaction in the tunnelling regime is shown in figure 1.

Intense short laser pulse ionises the cluster atoms and makes a nanoplasma sphere. Quasifree electrons participate in oscillation that is formed by the femtosecond laser pulses and interact with other particles to produce additional free electrons and vacancies in the inner shell leading to X-ray radiation. Many electrons in the find enough energy to escape from the cluster and leave behind a net positive charge. Then, the cluster expands in response to Coulomb explosion and hydrodynamic forces. At this time, the ponderomotive force and hydrodynamic pressure of electrons play significant roles in accelerating the electrons.

2.3 Ionisation of clusters

When the rising edge of the laser pulse gets to the cluster, ionisation of the cluster begins and a small number of quasifree electrons are generated, and this phenomenon is called the tunnel ionisation. The rate of tunnel ionisation, W_{ADK} , found by Ammosov, Delone and Krainov is described by the ADK formula [25]. Thereafter, a few electrons produced by optical ionisation collide with atoms and create another ionisation that is called collisional ionisation and its ionisation rate, W_{col} , in the nanoplasma model is calculated by the Lotz equation [26]. The electrons in the cluster have a velocity associated with their oscillations in the laser field. This oscillation leads to another ionisation, the rate of which

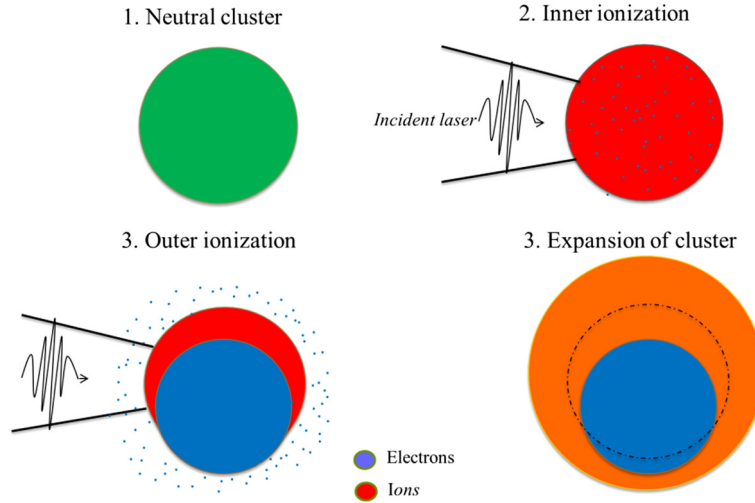


Figure 1. Stages of the cluster dynamics.

is W_{las} [27]. Then, the total ionisation rate of the laser–cluster interaction is

$$W = W_{\text{ADK}} + W_{\text{col}} + W_{\text{las}}. \quad (5)$$

The released electrons can be recombined with ions and thereby release energy. The rate of three-body recombination, α_3 , which reduces the electron density and increases the cluster heat is given by [28–30]

$$\alpha_3 = \frac{4\pi\sqrt{2\pi}}{9} \frac{e^{10}Z^3}{m_e^{1/2}(kT_e)^{9/2}} \ln\sqrt{1+Z^2}. \quad (6)$$

Here, Z is the charge state of the cluster.

2.4 Heating of the cluster

The nanoplasma model provides an explanation for the higher ion energies generated from large clusters compared to molecules and small clusters in terms of highly efficient collisional heating (inverse Bremsstrahlung) in the high-density nanoplasma, as is seen in solid target laser plasmas. The above-threshold ionisation heating is also included, but its contribution is small (<100 eV). The collisional heating of the cluster is calculated in the nanoplasma model when heating of a uniform dielectric sphere occurs in the time-varying electric field of the laser. Inside the cluster, the electric field is [28]

$$E = \frac{3}{|\varepsilon + 2|} E_0. \quad (7)$$

Here, E_0 is the external field and the plasma dielectric constant is given by the Drude model

$$\varepsilon = 1 - \frac{n_e/n_{\text{crit}}}{1 + i\nu/\omega}, \quad (8)$$

where n_e and n_{crit} are the electron density and critical plasma density, ω is the laser frequency and ν is the electron–ion collision frequency that is calculated from the Silin formulae [29]. When $n_e = 3n_{\text{crit}}$, $|\varepsilon + 2|$ will be minimum and the field inside the cluster gets larger. At this time, the cluster heating rate is also increased, even though the electron–ion collision frequency is actually reduced. The electron temperature equation inside the cluster is given by [30,31]

$$\frac{\partial T_e}{\partial t} = \frac{2}{3} \frac{Q}{n_e} - \frac{T_e}{n_e} \frac{dn_e}{dt} + \frac{2}{3} \sum_{Z=0}^{\infty} \varepsilon_i(Z) \times [\alpha_3(Z+1)n_en_i(Z+1) - S(Z)n_i(Z)]. \quad (9)$$

Here, n_e is the electron density, S is the collisional ionisation rate coefficient, Q is the absorption rate for a clustered plasma and α_3 is the rate of three-body recombination, which are effective parameters in electron temperature. After the initial ionisation, the electron density in the cluster plasma is much larger than the critical density.

2.5 Expansion of clusters

Cluster expansion is the result of Coulomb pressure and hydrodynamic pressure inside the cluster in the nanoplasma model. Coulomb pressure is due to the repulsion of ions within the clusters. The hydrodynamic pressure is the result of the expansion of hot electrons that is given by

$$P_e = n_e k T_e. \quad (10)$$

Here T_e is the electron temperature, n_e is the electron density and k is the Boltzmann constant. To expand the spherical cluster with uniform atoms, the principle of

conservation of energy implies that the rate of work that the pressure applied on the sphere must be equal to the change in the total kinetic energy of the system. Therefore, one get

$$P4\pi r^2 \frac{\partial r}{\partial t} = \frac{\partial K_c}{\partial t}. \quad (11)$$

Here K_c is the total kinetic energy and r is the cluster radius.

2.6 Effective force (ponderomotive force)

When a beam of high-power laser radiation is used to heat the plasma, radiation pressure becomes very important. By ponderomotive force of the laser light called effective force, the electrons in the plasma are accelerated to relativistic energies. In hydrodynamic model, plasma dynamics are driven predominantly by the hydrodynamic pressure and the ponderomotive pressure. The enhancement of the laser intensity at the critical density surface, initial ions density of the cluster and shape of the laser pulse make ponderomotive forces an important component of the plasma dynamics. The equation of motion of electrons in the presence of an EM wave is described by

$$\vec{F}_L = m \frac{d\vec{v}}{dt} = -e(\vec{E}(\vec{r}, t) + \frac{1}{c} \vec{U} \times \vec{B}(\vec{r}, t)), \quad (12)$$

where $\vec{E}(\vec{r}, t)$, \vec{U} and $\vec{B}(\vec{r}, t)$ are the electric field, electron velocity and magnetic field, respectively. The electric field is given by

$$\vec{E}(\vec{r}, t) = \vec{E}_s(\vec{r}) f(t) \cos \omega_0 t. \quad (13)$$

Here, $f(t)$ and ω_0 denote the temporal profile and the carrier frequency, respectively. A Gaussian envelope of $f(t)$ is given by

$$f(t) = \exp\left[-\frac{2 \ln 2 t^2}{\tau^2}\right], \quad (14)$$

where τ is the FWHM time duration. Linearly chirped laser field can be defined as follows:

$$E(t) = E_0 \exp\left\{-\left(1 + ib\right) \left(\frac{t\sqrt{2 \ln 2}}{\tau_L}\right)^2\right\}, \quad (15)$$

where b and τ_L are the chirp parameter and pulse duration. $b > 0$ means a positive chirp, $b < 0$ means a negative chirp and $b = 0$ means a Gaussian pulse. Laser intensity of the chirped laser pulse is expressed as follows:

$$I(t) = I_0 \exp\left\{\left[-\frac{t^2}{2\tau^2}\right] \left[1 + \frac{bt}{(t^2 + \tau^2)^{1/2}}\right]^{-1}\right\}, \quad (16)$$

where I_0 denotes the peak laser intensity of the near transform limited pulse. By using a second-order approximation and expansion of E around r_0 , the force exerted on an electron can be obtained as follows:

$$\vec{F}_{NL} = -\frac{\omega_p^2}{8\pi\omega_0^2} \vec{\nabla} \langle \vec{E}^2 \rangle. \quad (17)$$

Although this force essentially enters the electrons, in the end, it is transmitted to the ions too. The direction of this force is along the spatial gradients of the laser field. When electrons are classified by \vec{F}_{NL} , a field separator (\vec{E}_{es}) is produced. Therefore, the total force, which is the same ponderomotive force exerted on the electrons, would be as follows:

$$\vec{F}_e = -e\vec{E}_{es} + \vec{F}_{NL}. \quad (18)$$

Indeed, the ponderomotive force is very important for accelerating electrons and ions.

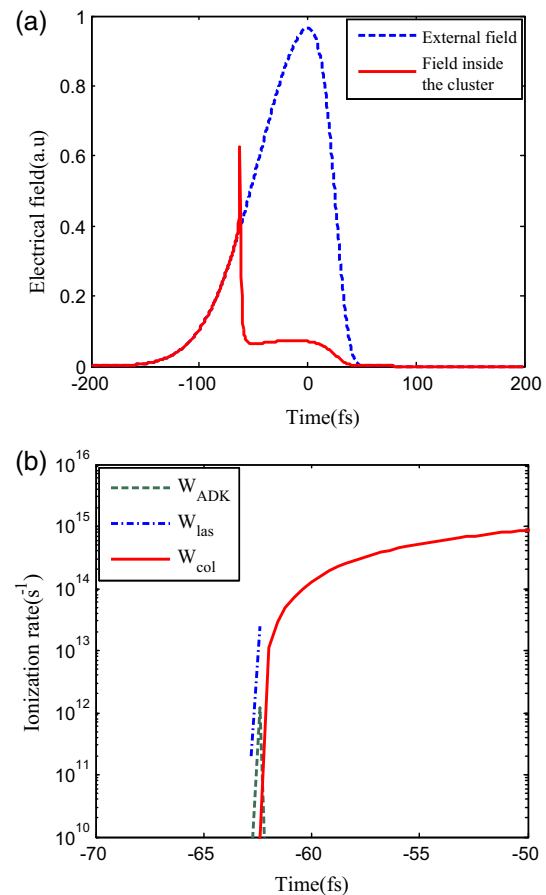


Figure 2. (a) Time evolution of the field inside the cluster and the external chirp intense laser pulse field and (b) rates of ADK ionisation, collisional ionisation, and laser-assisted ionisation for $\text{Ar} \rightarrow \text{Ar}^+$ during the short period of field enhancement. $I = 1 \times 10^{15} \text{ W cm}^{-2}$, $\lambda = 800 \text{ nm}$, $\tau = 40 \text{ fs}$.

3. Results

This paper considers the interaction of femto-second laser pulses with argon clusters for computational results. Three laser pulse shapes: Gaussian pulse, positively and negatively chirped laser pulses are used for interaction in the intensities of 10^{14} – 10^{17} W cm⁻². Argon cluster radius is considered to be 15 nm and the laser wavelength is 800 nm. The simulation of this laser–cluster interaction is carried out by particle-in-cell (PIC) method in one dimension. The systems of ordinary differential equations are solved numerically using a Runge–Kutta solver in GNU Scientific Library (GSL).

The enhanced field and ionisation rates for different mechanisms are shown in figure 2. When intensity increases, n_e rises as a result of the increased tunnel ionisation rate. When n_e approaches $3n_{crit}$, then the internal field increases resulting in an increase in ionisation rate. Figure 2a shows that at $t = -62.4$ fs, the field inside the cluster reaches its maximum value and W_{ADK} and W_{las}

begin to increase leading to the increase of the collisional ionisation rate. Figure 2b shows that after this moment, collisional ionisation is the dominant mechanism of the three mentioned mechanisms in the interaction. Therefore, collisional ionisation is one of the most important mechanisms for generating electrons and increasing the electron density in the laser–cluster interaction. The origin of the time is selected in such a way that E_{ext} maximum is located at $t = 0$ with a FWHM of 40 fs.

The effect of laser pulse shapes on ionisation rate and electron temperatures is shown in figures 3. Figures 3a–3c show that by applying a negatively chirped laser pulse, tunnel ionisation start earlier. So, in the interaction of a negatively chirped laser pulse, other ionisations start sooner too. The high ionisation rate in the positively chirped pulse causes the density of ionised electrons to increase and this is presented in figure 5. It also appears from figure 3d that, when a negatively chirped laser pulse interacts with an atomic cluster, the electrons gain more energy than other states.

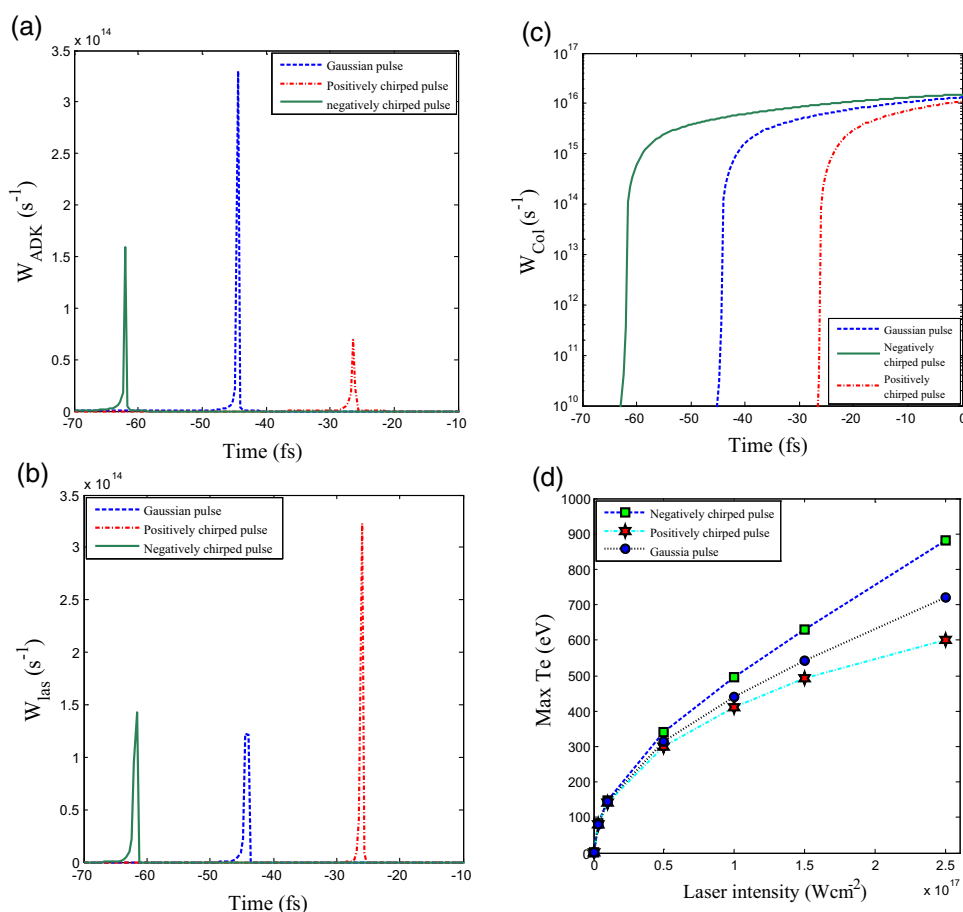


Figure 3. (a) Time evolution of the tunnel ionisation at different laser pulse shapes, (b) time evolution of the laser field ionisation at different laser pulse shapes, (c) time evolution of the collisional ionisation at different laser pulse shapes for a cluster irradiated by a 40 fs, 800 nm and 1×10^{15} W cm⁻² pulse, and (d) the variations in the maximum electron energy at different laser pulse shapes in different laser intensities with 40 fs duration pulse and 800 nm wavelength.

To provide more accelerated particles, the effect of the initial ion density and the laser pulse shape as the main effective parameters have been investigated on the electron energy. The strong dependence of the energy of electrons on the initial atomic density of the cluster is shown in figure 4. Figures 4a and 4b show that, by reducing the density of the cluster ions, electron temperature is increased. This is interpreted from eq. (9) which says that, by reducing the electron density, electron temperature increases. Thus, one can change the initial conditions of the rare gas within the gas jet and alter the nozzle geometry to present the cluster with less initial atomic density.

It is also clear that at low densities of the cluster atoms, when the positively chirped laser pulse interacts with the cluster, more energetic electrons are generated. But in high densities, high-energy electrons are obtained by negatively chirped laser pulse. In addition, by changing the shape of the laser pulse by chirping, the electron temperature increases further. As a result, one can obtain high-energy electrons with negatively chirped laser pulse (see figure 4b). This optimisation provides higher temperature which is beneficial for fast ignition. The dependence of the generated density of electrons on different initial ion density and different laser pulse shapes are shown in figure 5.

Figure 5a indicates that the ionisation process starts simultaneously for various initial ion densities. Moreover, figures 5b and 5c show that when the laser pulse interacts with the cluster, more electrons are released as a result of the increase in the number of atoms in the cluster, and consequently, more laser energy is spent on the ionisation of more electrons in the cluster leading to less energy gain by electrons. On the other hand, reducing the electron density with less initial ion density indicates that strong heating is dominant. Therefore, the electron density has a crucial role at the total temperature in the laser–cluster interaction. Furthermore, when the cluster is exposed to irradiation with positively chirped laser pulse, maximum density of electrons is high compared to the other pulse shapes. Because the electron pressure depends on electron density in accordance with eq. (10), there is an improvement for electron pressure which is evaluated by positively chirped laser pulse.

In order to obtain an estimate of the enhancement of the particle acceleration, the effect of laser intensity, initial ion density and the laser pulse shape have been investigated as the main parameters affecting the hydrodynamic pressure. Time evolution of the hydrodynamic pressure for different laser pulse shapes at $1 \times 10^{16} \text{ W cm}^{-2}$ laser intensity and the changes

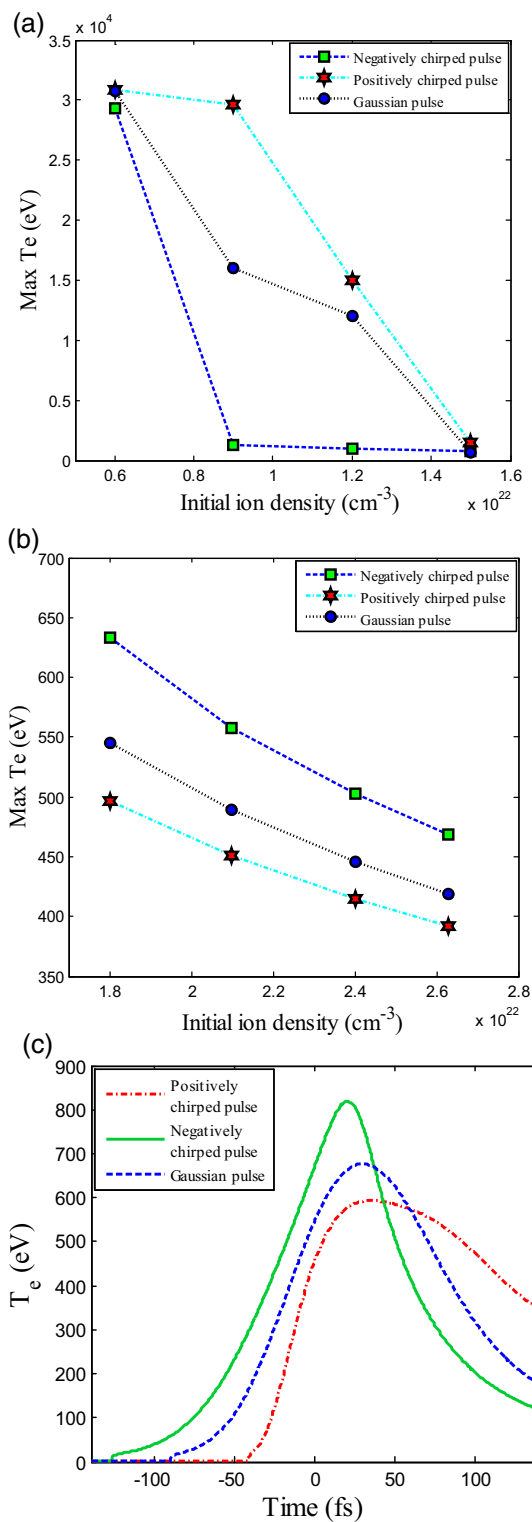


Figure 4. (a) Computed maximum energy of electrons vs. initial cluster atomic density at low densities, (b) computed maximum energy of electrons vs. initial cluster atomic density at high densities and (c) time evolution of electron temperature in different pulse shapes for a cluster irradiated by a 40 fs, 800 nm, $9 \times 10^{16} \text{ W cm}^{-2}$ pulse.

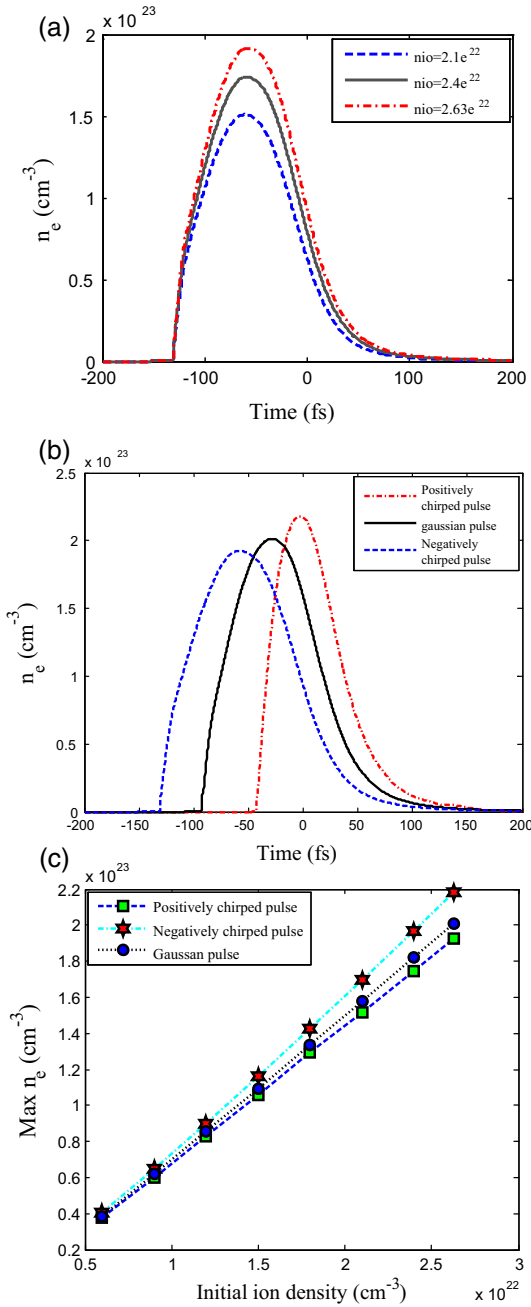


Figure 5. (a) Time evolution of the electron density at different initial ion density, (b) time evolution of the electron density in different pulse shapes for a cluster irradiated by a 40 fs, 800 nm and $2.4 \times 10^{17} \text{ W cm}^{-2}$ pulse, and (c) the maximum electron density vs. initial cluster atomic density.

of the maximum hydrodynamic pressure at different initial ion density and laser intensities are shown in figure 6. Based on figure 6a, when the cluster is exposed to irradiation with positively chirped laser pulse, electron pressure is more than that of the Gaussian pulse and negatively chirped pulse. It should be mentioned that the hydrodynamic pressure of electrons play an important role in the acceleration of electrons. It is evident

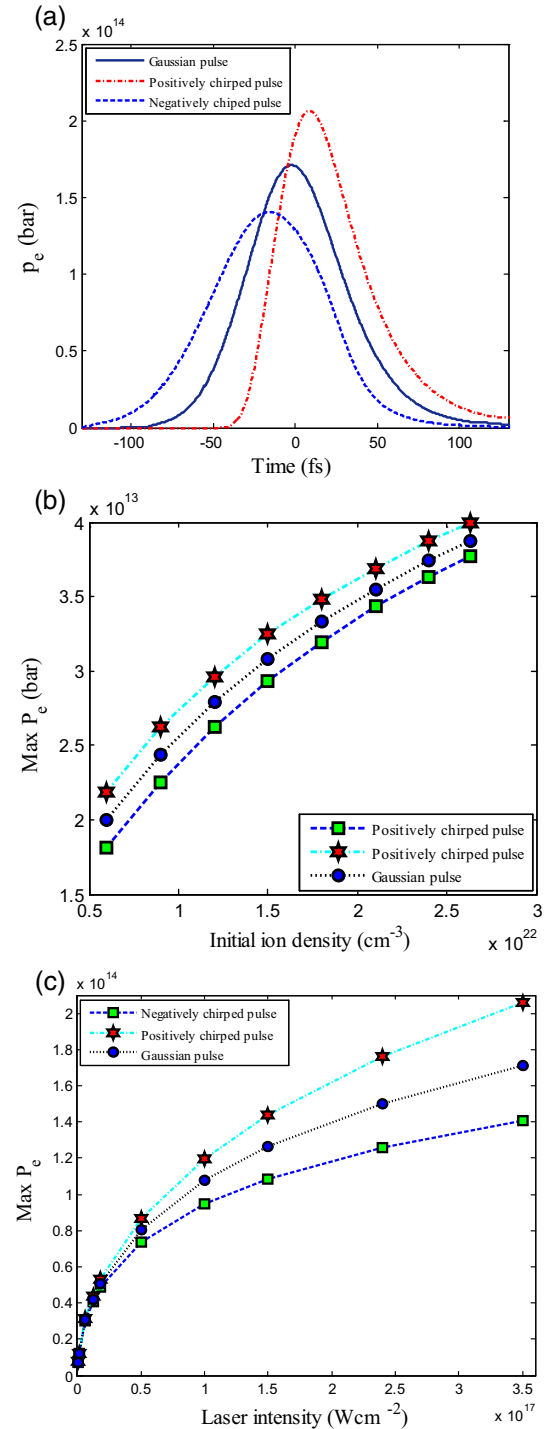


Figure 6. (a) Time evolution of the hydrodynamic pressure for a cluster irradiated by 40 fs, 800 nm and $2.4 \times 10^{17} \text{ W cm}^{-2}$ pulse, (b) maximum electron pressure vs. initial cluster atomic density in an Ar cluster irradiated by different laser pulse shapes and (c) the computed maximum electron pressure vs. laser intensity.

from figure 6b that the increase in the initial ion density causes an increase in the electron pressure. Although the electron temperature in the laser–cluster interaction with negatively chirped laser pulse is high, the

electron pressure is high with positively chirped pulse. This happens because electrons will have maximum density with positively chirped laser pulse. Therefore, the density of electron increases more than the temperature of the electrons with positively chirped laser pulse and hydrodynamic electron pressure with positively chirped laser pulse will also be high in accordance with eq. (10). In addition, it is clear from eq. (9) that different mechanisms such as tunnelling ionisation, collisional ionisation, field ionisation, recombination of the electrons and the inverse bremsstrahlung (IBS) absorption rate play important roles in the electron pressure. Likewise, the electron pressure increases as a result of the increase in the density of initial atoms in the cluster. In the case of large clusters which are exposed to irradiation by moderate intensities, the fraction of electrons leaving the clusters is negligible. The Coulomb pressure is, therefore, ignored and electron hydrodynamic pressure is the single pressure inside the cluster. Figure 6c shows that increasing laser intensity causes considerable increase in the electron pressure. Hence, with this modification the electron pressure is improved by about 22%. This can have good impact on many of the applications of laser–cluster interaction such as laser plasma accelerators.

4. Conclusion

The response of argon cluster to femtosecond laser pulses with intensity of 10^{15} – 10^{17} W cm⁻², pulse duration of 40 fs and wavelength of 800 nm was examined. Calculation was extended with nanoplasma model in order to modify ionisation process, heating and expansion of a cluster by different laser pulse shapes, the positively and negatively chirped laser pulse and Gaussian pulse. This simulation is focussed basically on the evolution of electric field inside the cluster, ionisation mechanisms, electron density and electron pressure. In addition, the effects of laser intensity and initial atomic cluster on the electron pressure and electron density were investigated. The main achievement was the detection of laser pulse chirp effect on the electron density and hydrodynamic pressure. It is found that electron density is considerably increased when the cluster bunch interacts with positively chirped laser pulse, leading to the escalation in the hydrodynamic pressure inside the cluster. The results show that the electron pressure is improved by about 22 percent. This plays a significant role in accelerating the electrons resulting in the system's energy and temperature enhancement that may be beneficial for laser application in fast ignition and fusion.

References

- [1] D Strickland and G Mourou, *Opt. Commun.* **55(6)**, 447 (1985)
- [2] R Sadighi-Bonabi, E Irani, B Safaie, K Imani, M Silatani and S Zare, *Energy Convers. Manag.* **51(4)**, 636 (2010)
- [3] L Chen, M Kando, M H Xu, Y T Li, J Koga, M Chen, H Xu, X H Yuan, Q L Dong, Z M Sheng and S V Bulanov, *Phys. Rev. Lett.* **100(4)**, 045004 (2008)
- [4] H Ghaforyan, M Ebrahimzadeh, T Ghaffary, H Reza-zadeh and Z S Jahromi, *Chin. J. Phys.* **52(1)**, 233 (2014)
- [5] R Sadighi-Bonabi, H Hora, Z Riazi, E Yazdani and S K Sadighi, *Laser Part. Beams* **28(1)**, 101 (2010)
- [6] R Sadighi-Bonabi, F W Lee and C B Collins, *J. Appl. Phys.* **53(12)**, 8508 (1982)
- [7] H Ghaforyan, R Sadighi-Bonabi and E Irani, *Adv. High Energy Phys.* **2016**, 1 (2016)
- [8] X Qi and W Lin, *Pramana – J. Phys.* **88(2)**: 35 (2017)
- [9] S Rasti, E Irani and R Sadighi-Bonabi, *AIP Adv.* **5(11)**, 117105 (2015)
- [10] K W Ledingham, P McKenna and R P Singhal, *Science* **300(5622)**, 1107 (2003)
- [11] B Cui, B Tang, R Ma, Q Huang, Y Ma, L Chen and W Jiang, *Rev. Sci. Instrum.* **83(2)**, 02A321 (2012)
- [12] E Yazdani, R Sadighi-Bonabi, H Afarideh, Z Riazi and H Hora, *J. Appl. Phys.* **116(10)**, 103302 (2014)
- [13] S Zare, E Yazdani, R Sadighi-Bonabi, A Anvari and H Hora, *J. Appl. Phys.* **117(14)**, 143303 (2015)
- [14] F N Beg, K Krushelnick, C Gower, S Torn, A E Dargor, A Howard, T Sumner, A Bewick, V Lebedenko, J Dawson and D Davidge, *Appl. Phys. Lett.* **80(16)**, 3009 (2002)
- [15] V D Zvorykin, A O Levchenko, A V Shutov, E V Solomina, N N Ustinovskii and I V Smetanin, *Phys. Plasmas* **19(3)**, 033509 (2012)
- [16] N L Kugland, B Aurand, C G Brown, C G Constantin, E T Everson, S H Glenzer, D B Schaeffer, A Tauschwitz and C Niemann, *Appl. Phys. Lett.* **101(2)**, 024102 (2012)
- [17] L Zhang, L M Chen, W M Wang, W C Yan, D W Yuan, J Y Mao, Z H Wang, C Liu, Z W Shen, A Faenov and T Pikuz, *Appl. Phys. Lett.* **100(1)**, 014104 (2012)
- [18] T Ditmire, T Donnelly, A M Rubenchik, R W Falcone and M D Perry, *Phys. Rev. A* **53(5)**, 3379 (1996)
- [19] S Micheau, H Jouin and B Pons, *Phys. Rev. A* **77(5)**, 053201 (2008)
- [20] O F Hagena and W Obert, *J. Chem. Phys.* **56(5)**, 1793 (1972)
- [21] C Rose-Petrucci, K J Schafer, K R Wilson and C P Barty, *Phys. Rev. A* **55(2)**, 1182 (1997)
- [22] I Last and J Jortner, *Phys. Rev. Lett.* **87(3)**, 033401 (2001)
- [23] D Brunner, H Angerer, E Bustarret, F Freudenberg, R Höpler, R Dimitrov, O Ambacher and M Stutzmann, *J. Appl. Phys.* **82(10)**, 5090 (1997)
- [24] H M Milchberg, S J McNaught and E Parra, *Phys. Rev. E* **64(5)**, 056402 (2001)
- [25] M V Ammosov, N B Delone and V P Krainov, *J. Exp. Theor. Phys.* **64(6)**, 1191 (1986)

- [26] W Lotz, *Z. Phys. A* **232**(2), 101 (1970)
- [27] J S Zweiback, *Resonance effects in laser cluster interactions*, Ph.D. dissertation (University of California, Davis, 1999)
- [28] J D Jackson, *Classical electrodynamics* (Wiley, New York, 1975) Vol. 523
- [29] V P Silin, *Sov. Phys. JETP* **20**(6), 1510 (1965)
- [30] O F Kostenko and N E Andreev, *Plasma Phys. Rep.* **33**(6), 503 (2007)
- [31] A F Haught, W B Ard, W J Fader, R A Jong, A Sing, D H Polk, R G Tomlinson and J T Woo, *Fifth Conference Proceedings* (Tokyo, 1974) p. 391